ELSEVIER

Thermochimica Acta 319 (1998) 185–191

thermochimica
acta

A DSC study on thermoxidation kinetics of mustard oil

G. Litwinienko*, T. Kasprzycka-Guttman

Department of Chemistry, Warsaw University, Pasteura 1, 02-093 Warsaw, Poland

Received 5 January 1998; received in revised form 28 May 1998; accepted 8 June 1998

Abstract

Mustard oil was studied by non-isothermal DSC to determine the kinetic parameters of thermal oxidation. Values of the first and second maxima of heat flow and the point of the extrapolated onset of the exothermic process obtained at different heating rates were used to calculate activation energies and Arrhenius kinetic parameters of thermal-oxidative decomposition of the oil, using the Ozawa–Flynn–Wall (OFW) method. The calculated activation energies 90.6±6.2 (for onset of oxidation), 88.5±2.8 (for first peak) and 84.6±1.1 kJ/mol (for second peak) were used for calculating the DSC signal. The following complex reaction models were examined: multiple reaction; competitive reaction; sequential reaction; and sequential reaction with autocatalysis start. The best fit was observed for the two-step autocatalytic reaction and the influence of the mechanism of oil autoxidation on the shape of the measured DSC signal was confirmed by this model. © 1998 Elsevier Science B.V.

Keywords: Activation energy; Autoxidation; DSC; Edible oils; Kinetics of thermoxidation; Mustard oil

1. Introduction

The autoxidation of edible oils is one of the most important problems in food storage and oil processing technology. The autoxidation process is a chain reaction and can be described by equations where RH denotes the lipid molecule:

Initiation:

$$\text{Initiator} \longrightarrow \text{Product of initiation/radicals}$$

Propagation:

$$R^{\cdot} + O_2 \xrightarrow{k_1} RO_2$$

$$RO_2^{\cdot} + RH \xrightarrow{k_2} ROOH + R^{\cdot}$$

Termination:

$$RO_2^{\cdot} + RO_2^{\cdot} \xrightarrow{k_3}$$

$$RO_2^{\cdot} + R^{\cdot} \xrightarrow{k_4}$$

$$R^{\cdot} + R^{\cdot} \xrightarrow{k_5}$$

Radicals recombination products

The oxidation of lipids has been the subject of many

---

*Corresponding author. Fax: +4822 822 59 96; e-mail: litwin@chem.uw.edu.pl

PII S0040-6031(98)00410-9

researches, based on the determination of peroxide concentrations, volumetric methods (measurement of oxygen consumption), chemiluminescent methods and thermoanalytical methods.

Kissinger [1] and Ozawa and Flynn [2,3] demonstrated that differential scanning calorimetry (DSC) technique, based on the linear relation between peak temperature and heating rate, can be used to determine the kinetic parameters of reaction (activation energy, rate constant). These methods and their modified versions [4,5] are widely used for the investigation of thermal decomposition of organic materials, polymers and petroleum products. Studies by Pereira [6], Wesolowski [7], Kowalski [8,9] and our previous experiments [10,11] showed that the isothermal and non-isothermal DSC techniques can be successfully applied to the analysis of autoxidation of edible oils. Isothermal calorimetry experiments are rather time-consuming and are usually carried out under high pressure of oxygen (pressure differential scanning calorimetry). In contrast, non-isothermal calorimetry experiments are much faster and can give more information, not only about the first step of oxidation (observed in conventional isothermal methods), but also further steps of oxidation from a single run. Although, many researchers use non-isothermal calorimetry methods, the complicated nature of oxidation phenomena during linear programmed heating has not been explained. This paper concentrates on the mathematical interpretation of experimentally measured data. These theoretical considerations about complex reactions can add to the explanation of the shape of the non-isothermal DSC curve of oxidation.

Examining the nature of multiple reactions, Agrawal [12–14] proposed mathematical procedures describing the theoretical behaviour of complex reactions as a function of heating rate. The temperature interval of chemical changes and the nature of the overall complex reaction is a function of the kinetic parameters of individual reactions. Procedures described in [13,14] were used in this paper for computer simulation of mustard oil autoxidation. The following kinds of complex reactions were taken into consideration: (1) competitive reactions; (2) multiple reactions; (3) sequential reactions; and (4) sequential reactions with autocatalysis.

1.1. Competitive reactions

This reaction includes parallel–competitive reactions:

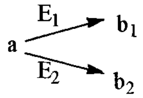

(1)

where; a represent reactant a, b_1 and b_2 the products. For different heating rates β, the rate of reaction Eq. (1) can be evaluated from the following expression:

$$-\frac{\mathrm{d}a}{\mathrm{d}T}=\frac{a}{\beta}\sum A_i\exp\left(-\frac{E_i}{RT}\right) \tag{2}$$

where a denotes the amount of reactant a, E_i the activation energy, A_i the pre-exponential factor and R the gas constant.

1.2. Multiple reaction

$$a_1 \rightarrow b_1 \tag{3}$$
$$a_2 \rightarrow b_2$$

Subscripts (1,2) are used to identify the individual reactions. The individual reaction rate is presented as:

$$-\frac{\mathrm{d}a_i}{\mathrm{d}T}=\frac{a_iA_i}{\beta}\exp\left(-\frac{E_i}{RT}\right) \tag{4}$$

The overall multiple reaction rate is represented by:

$$\frac{\mathrm{d}a}{\mathrm{d}T}=\sum_{i=1}^{n} g_i\frac{\mathrm{d}a_i}{\mathrm{d}T} \tag{5}$$

and

$$a=\sum g_ia_i \tag{6}$$

where, g_i is the weight factor and $\sum g_i=1$.

1.3. Sequential reaction scheme

$$a\overset{E_1}{\rightarrow}b\overset{E_2}{\rightarrow}c \tag{7}$$

where c may be a gaseous product of thermoxidation and the rate expressions are given by:

$$-\frac{\mathrm{d}a}{\mathrm{d}T}=\frac{A_1a}{\beta}\exp\left(-\frac{E_1}{RT}\right) \tag{8}$$

$$\frac{\mathrm{d}b}{\mathrm{d}T}=-\frac{\mathrm{d}a}{\mathrm{d}T}-\frac{A_2b}{\beta}\exp\left(-\frac{E_2}{RT}\right) \tag{9}$$

1.4. Sequential reaction scheme with autocatalysis

The reaction *a*—>*b* is accelerated by product *b*, formed in this reaction and the rate of consumption of substrate *a* is given by:

$$\frac{\mathrm{d}a}{\mathrm{d}T}=-\frac{A_1ab}{\beta}\exp\left(-\frac{E_1}{RT}\right) \tag{10}$$

In this case, the expression for the rate, d*b*/d*T* is the same as in Eq. (9).

2. Experimental

2.1. Materials and apparatus

Commercial mustard oil was used. The fatty acids composition, determined by GLC analysis, is listed in Table 1.

A DuPont 910 differential scanning calorimeter with a DuPont 9900 thermal analyzer and a normal pressure cell were used in the dynamic method measurements. Calibration of the apparatus was carried out with a high purity indium standard. A 3–5 mg oil samples were placed in open aluminum sample pans and heated at the rates of 2, 5, 7.5, 10 and 15 K/min. Experiments were performed in an atmosphere of oxygen at a gas flow rate of 6 l/h. The determinations were made for each of the five programmed heating rates. The course of the experiment was monitored and analyzed by the DSC software.

Table 1
The fatty acid composition of mustard oil

Parameter	Value (%)			
	present work	references		
		[18]	[19]	[20]
Acid number[a]	5.17	–	–	–
Peroxide number[b]	14.35	–	–	–
$C_{16:0}$	2.5	2.4	2.2–2.3	0.5–4.5
$C_{16:1}$	0.4	0.3	0.2–0.3	0.5
$C_{18:0}$	0.6	0.8	0.6–0.8	0.5–2.0
$C_{18:1}$	25.5	26.3	18–25.7	8–23
$C_{18:2}$	9.8	10.4	8.9–10.9	10–24
$C_{18:3}$	12.6	12.1	9.5–11.1	6–18
$C_{20:0}$	1.4	1.3	0.4–0.7	1.5
$C_{20:1}$	8.9	9.1	8.1–11.6	5–13
$C_{22:0}$	34.5[c]	35.6[c]	0.15–0.3	0.2–2.5
$C_{22:1}$			35–47.8	22–50
$C_{22:2}$	1.2	1.1	0.05–0.2	<1

[a] In mg of KOH per gram of fat.

[b] Expressed in ml of 0.002 N thiosulphate per gram of fat.

[c] Collected value for $C_{22:0}$ and $C_{22:1}$.

2.2. Methods

The method used in the analysis of mustard oil was based on DSC experiments in which the temperatures of the extrapolated onset of the thermoxidation process (T_e) and temperatures of maximum heat flow (T_p) were determined from the resulting measured curves for exothermic reactions. Typical curves for mustard oil are shown in Fig. 1. The temperatures of the two peaks, T_{p1}, T_{p2}, and the extrapolated onset temperatures, T_e are listed in Table 2. All values are averages of at least three determinations. They were utilized to calculate kinetic parameters by the Ozawa–Flynn–Wall (OFW) method [2,3,15]. The activation energies, E_1 and E_2 (indexes 1 and 2 denotes first and second reactions), and pre-exponential factors, A_1 and A_2, were calculated from the temperatures of both the observed peaks on the DSC curves, T_{p1} and T_{p2}, respectively.

The plot of $\log\beta$ vs. $1/T_p$, found by the OFW method, shows the linear dependence described by the following:

$$\log\beta = aT_p^{-1}+b \tag{11}$$

which is also valid for T_e, where β is the heating rate.

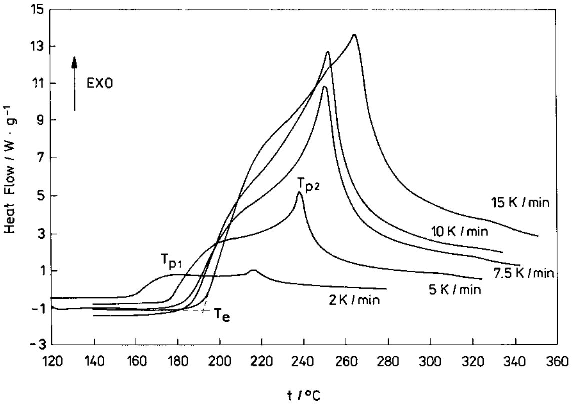

Fig. 1. DSC curves of thermal oxidation of mustard oil: heating rates 2, 5, 7.5, 10 and 15 K/min.

Table 2
Data obtained from DSC curves for mustard oil

β/(K/min)	T_e/K	T_{p1}/K	T_{p2}/K
2	429.8	452.7	490.9
5	448.7	470.8	512.8
7.5	453.6	478.1	523.4
10	457.0	–	530.7
15	465.4	–	540.6

Table 3
Parameters calculated by means of the Ozawa-Flynn-Wall method

Parameters	T_e	T_{p1}	T_{p2}
Slope	−4.975	−4.858	−4.646
Reciprocal	11.851	11.03	9.761
Standard error σ	0.045	0.013	0.008
E'(kJ/mol)	90.6	88.5	84.6
A (min^{-1})	3.48×10^9	1.49×10^9	4.46×10^7
k at 500 K (min^{-1})	0.97	0.90	1.12
$t_{1/2}$ at 500 K (min)	0.71	0.77	0.62

For each heating rate, the peak of DSC signal represents a system at the state of the same constant conversion [15]. The advantage of the OFW method is that the activation energy can be determined without knowing the kinetic model of the reaction [2,3,15,16]. The Arrhenius activation energy for the process and the pre-exponential factor Z can be written as:

$$E = -2.19R\frac{\mathrm{dlog}\,\beta}{\mathrm{d}T_{\mathrm{p}}^{-1}} \tag{12}$$

$$A = \frac{\beta E\exp\left[E/RT\right]}{RT_{\mathrm{p}}^{2}} \tag{13}$$

The temperature dependence of the specific rate constant k is described by the Arrhenius equation: $k{=}A\exp\left(-E/RT\right)$, where A is the pre-exponential factor, E the Arrhenius activation energy, R the gas constant and T the absolute temperature. The equation was used for the calculation of Arrhenius kinetic parameters and the activation energy of thermal-oxidative decomposition of oil. More information on the methodology and apparatus has been given previously [17].

3. Results and discussion

Fig. 1 shows the DSC plots obtained for five heating rates: 2, 5, 7.5, 10 and 15 K/min, in the range of 140°–320°C. All scans were similar to one another but, generally, the higher the heating rate, the higher the temperature of maximum heat flow. All kinetic parameters of thermoxidation, calculated by OWF method, are listed in Table 3.

The values of activation energy, calculated from the onset points and first peak, were 90.6±6.2 and 88.5±2.8 kJ/mol, respectively, and these were higher than the activation energies calculated from the second peak: 84.6±1.1 kJ/mol. The constant rate of reaction (k) and its half time ($t_{1/2}$) were obtained from equations describing the first-order reaction. In Fig. 1, which presents the results obtained experimentally, two peaks are visible. It suggests that two major processes occur. Taken together, the different values of E_a and the differences between the shapes of DSC curves indicate that at least two reactions took place. In such a process, at low heating rates and lower temperatures, one type of reaction may predominate over the other. In the case when the values of the activation energies are similar, it is not possible to distinguish between separate reactions in this process by variation of β.

The simulations were performed using the values of activation energies E and coefficients A calculated from the first maximum (E_a, A_a) and second maximum (E_b, A_b) of the heat flow. This procedure was expected to show which type of reaction (models 1–4) gave the results closest to the experimental ones.

3.1. Competitive reactions

The computer simulations based on Eq. (2) are presented in Fig. 2 and this model is inconsistent with the experimental data, since above the isokinetic temperature, T_{iso} (i.e. the temperature at which rates of two competitive processes are equal [14]; in this case, $T_{\mathrm{iso}}{=}184$ K), the first calculated peak becomes less pronounced. It indicates that one of these reactions should predominate (see reaction scheme 5) and calculations give only one maximum of heat flow at all examined heating rates. This calculation led to the conclusion that the competitive-reactions model cannot be applied to describe thermoxidation process.

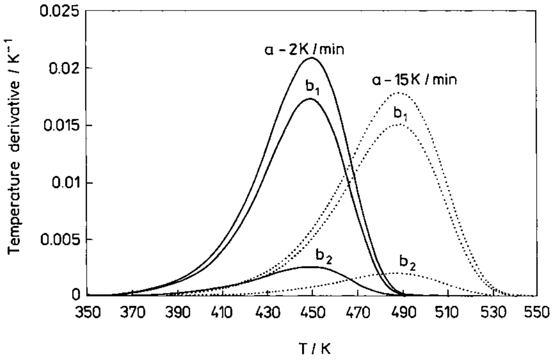

Fig. 2. Temperature derivative of increase of products (b_1 and b_2) and decrease of substrate a vs. temperature for competitive reaction at heating rates of 2 and 15 K/min.

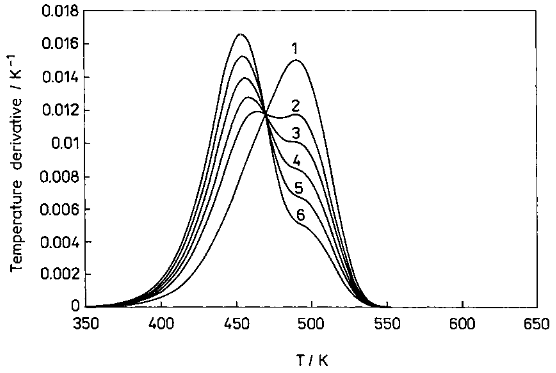

Fig. 3. Rate of overall reaction ($-\mathrm{d}a/\mathrm{d}T$) vs. temperature at a heating rate of 2 K/min for multiple-reaction model. Data for the initial composition of mixture: line 1 (g_1=0.1, g_2=0.9), line 2 (g_1=0.3, g_2=0.7), line 3 (g_1=0.4, g_2=0.6), line 4 (g_1=0.5, g_2=0.5), line 5 (g_1=0.6, g_2=0.4).

3.2. Multiple reaction

In order to simulate the multiple-reaction model (scheme 3), the calculations were performed for different compositions of oxidized oil (Fig. 3 lines 1–5, respectively). The temperature range in which the multiple reaction occurs is wider than that for the competitive reaction. We observed an insignificant dependence of composition of the starting mixture on the values of the calculated T_{p1} and T_{p2}. Multiple peaks in this simulated reaction were visible for $0.20<g_1/g_2<0.80$ at all the heating rates examined.

A good agreement between the experimental and simulated data was observed only for temperatures of both maxima and for g_1=0.4 and g_2=0.6. These values are shown in Table 4. In the analyzed mustard oil, the ratio of the unsaturated compounds/other compounds is 0.6/0.4 (see Table 1), i.e. in this simulation, unsaturated compounds react as a_2 in scheme (3) and can be characterized by the activation energy calculated from the second peak. However, the onset of the process is not consistent with our calculations.

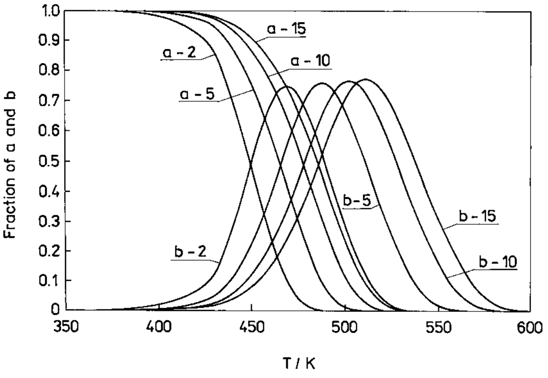

Fig. 4. Changes in normalized fractions of reactant a and product b as a function of temperature at heating rates 2, 5, 10 and 15 K/min for the sequential reaction scheme.

3.3. Sequential reaction scheme

Normalized participation of substrate a and the first product b in the reaction system is shown in Fig. 4. A summary of the rates of reactions taking part in the overall process vs. temperature for considered the sequential reaction scheme is shown in Fig. 5. The

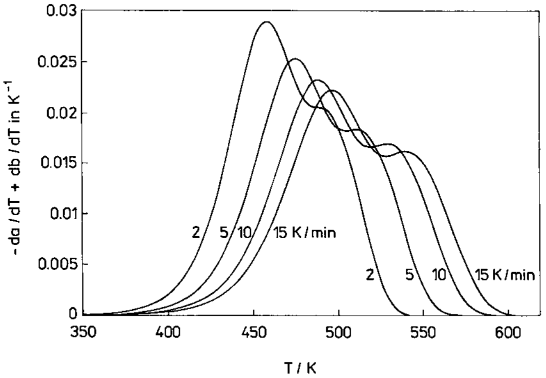

Fig. 5. Temperature derivative of reactants ($-\mathrm{d}a/\mathrm{d}T+\mathrm{d}b/\mathrm{d}T$) vs. temperature at heating rates 2, 5, 10 and 15 K/min for the sequential reaction scheme.

Table 4

Calculated and experimental values of temperatures in K, differences ΔT and relative errors δ (%) of multiple-reaction model for different heating rates β (K/min)

β	Peak 1				Peak 2				Onset			
	T_{calc}	T_{exp}	ΔT	δ	T_{calc}	T_{exp}	ΔT	δ	T_{calc}	T_{exp}	ΔT	δ
2	464	452.7	11.3	2.5	492	490.9	1.0	0.2	409	429.8	−21	−5.1
5	483	470.8	12.2	2.6	512.5	512.8	0.3	0.1	420	448.7	−29	−6.9
7.5	491	478.1	12.9	2.7	522	523.4	1.4	0.3	427	455.6	−28	−6.5
10	497	–	–	–	530	527.7	2.3	0.4	434	457.0	−23	−5.3
15	505	–	–	–	542	540.6	1.4	0.3	439	465.4	−26	−5.9

Table 5

Calculated and experimental values of temperatures in K, differences ΔT and relative errors δ (%) of sequential-reaction model for different heating rates β (K/min)

β	Peak 1				Peak 2				Onset			
	T_{calc}	T_{exp}	ΔT	δ	T_{calc}	T_{exp}	ΔT	δ	T_{calc}	T_{exp}	ΔT	δ
2	460	452.7	7.4	1.6	492	490.9	1.0	0.2	405	429.8	−24	−5.9
5	477	470.8	6.2	1.3	512	512.8	−0.8	−0.2	419	448.7	−30	−7.2
7.5	484	478.1	5.9	1.2	523	523.4	0.4	0.1	426	455.6	−31	−7.3
10	490	–	–	–	530	527.7	2.3	0.4	428	457.0	−29	−6.8
15	498	–	–	–	541	540.6	0.4	0.1	438	465.4	−27	−6.1

temperatures of maximum heating rates and temperatures from former calculations for a multiple reaction were compared with the experimental data in Table 5. The calculated and experimentally obtained values of the temperature maxima for the first and second peaks were highly correlated. In contrast, the calculated temperature of the onset of reaction was significantly lower than the experimentally obtained one. Observed discrepancies suggested that the onset of the simulated process had to be modified, so the sequential reaction scheme was modified by taking autocatalysis into consideration.

3.4. Sequential reaction scheme with autocatalysis

A concentration of peroxides was taken as 0.06 mol/mol from the measured peroxide number which was used as the initial concentration of b in Eqs. (9) and (10). The results obtained are presented in Table 6. The comparison of experimental and calculated values of the degree of conversion at increased temperature (see Fig. 6) shows good agreement for this model of complex reaction. The value of the onset point depends on peroxide concentration. An approxi-

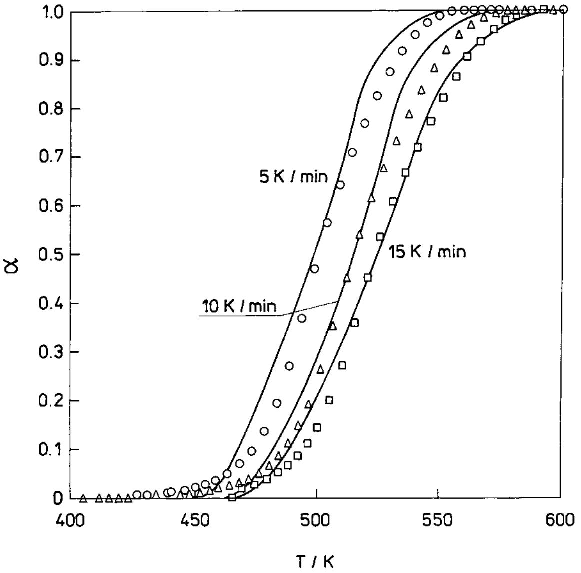

Fig. 6. Comparison of conversion as a function of temperature at heating rates 5, 10 and 15 K/min. (———) Experimental data, (· · ·) calculated data for sequential reactions with autocatalytic start.

Table 6
Calculated and experimental values of temperatures in K, differences ΔT and relative errors δ (%) of sequential-reaction model with autocatalysis at different heating rates β (K/min)

β	Peak 1				Peak 2				Onset			
	T_{calc}	T_{exp}	ΔT	δ	T_{calc}	T_{exp}	ΔT	δ	T_{calc}	T_{exp}	ΔT	δ
2	466	452.7	14	3.1	492	490.9	1	0.2	421	429.8	9	2.1
5	482	470.8	11	2.3	514	512.8	1	0.2	445	448.7	4	0.9
7.5	491	478.1	13	2.7	523	523.4	0	0	451	455.6	5	1.1
10	496	–	–	–	530	527.7	3	0.6	448	457.0	9	2.0
15	504	–	–	–	543	540.6	2	0.4	457	465.4	8	1.7

mated model of the sequential reactions with autocatalytic onset is the best explanation of the shape of the DSC signal and this model is in good agreement with the chain reaction scheme of free radical oxidation of lipids. This model shows that the first observed process in the non-isothermal DSC curve is caused by formation of peroxides. The second peak results from the decomposition of the peroxides to further products. Therefore, evaluation of the stability of edible oils using DSC by calculations of kinetic parameters of thermoxidation should consider the temperatures of the onset of the process and temperatures of the first rather than the second peak. Arrhenius activation energies and rate constants calculated from the onset and first peak may be useful in assessing the susceptibility of edible oils to oxidation.

Concluding, these experiments and calculations shows that onset of the thermoxidation process may be a very useful point for the determination of the effects of additives, such as pro- and antioxidants.

Acknowledgements

This work was supported by the BST-592/32/98.

References

[1] H.E. Kissinger, Anal. Chem. 29 (1957) 1702.
[2] T. Ozawa, J. Therm. Anal. 2 (1970) 301.
[3] J.H. Flynn, Thermochim. Acta 4 (1966) 323.
[4] J.H. Sharp, Reaction kinetics, in: Mackenzie (Ed.), Differential Thermal Analysis, 1972 p. 47.
[5] M.J. Starink, Thermochim. Acta 288 (1996) 97.
[6] T.A. Pereira, N.P. Das, Thermochim. Acta 165 (1990) 129.
[7] M. Wesołowski, Sci. Pharm. 54 (1986) 11.
[8] B. Kowalski, Thermochim. Acta 156 (1989) 347.
[9] B. Kowalski, Pol. J. Food Nutr. Sci., 1/42 (1992) 51.
[10] T. Kasprzycka-Guttman, D. Odzeniak, Thermochim. Acta 204 (1992) 303.
[11] G. Litwinienko, T. Kasprzycka-Guttman, M. Jarosz-Jarszewska, J. Therm. Anal. 45 (1995) 741.
[12] R.K. Agraval, Thermochim. Acta 128 (1988) 185.
[13] R.K. Agraval, Thermochim. Acta 203 (1992) 93.
[14] R.K. Agraval, Thermochim. Acta 203 (1992) 111.
[15] T. Ozawa, Thermochim. Acta 203 (1992) 159.
[16] J. Opfermann, E. Kaiserberger, Thermochim. Acta 203 (1992) 167.
[17] T. Kasprzycka-Guttman, M. Jarosz-Jarszewska, G. Litwinienko, Thermochim. Acta 250 (1995) 197.
[18] L. Appelgwist, R. Ohlsen, Rapeseed, Elsevier, Amsterdam, 1972, p. 186.
[19] F.G. Sietz, Fette, Seifen, Anstrichmittel 74(2) (1972) 72.
[20] G.F. Spencer, J. Am. Oil Chem. Soc. 53 (1976) 94–96.